Magnetic properties and short-range order in Co-Nb-B alloys

B. W. Corb* and R. C. O'Handley
Department of Materials Science and Engineering, Massachusetts Institute of Technology, Cambridge, Massachusetts 02139
(Received 9 October 1984)

The saturation magnetizations, crystallization temperatures, and thermomagnetic curves of various Co-rich Co-Nb-B glasses are presented. The saturation magnetizations and the phases of the crystallized specimens are also reported. A scanning transmission electron microscopy study on one of the glasses revealed no gross chemical phase separation. A model for the magnetic moments of a Co-T_E-M system is developed, with the use of Cowley's short-range order parameters, that is based on the coordination number of Co atoms around the early-transition-metal (T_E) and metalloid (M) atoms. Application of the model to the moment data shows that the coordination numbers around the Nb and B atoms in the glasses are 12 and 6, respectively, and that the Nb and B atoms have a tendency to cluster around each other. The moment difference between the crystalline and glassy samples may have been caused by Co_3Nb Laves-type phases present in the former, rather than by chemical phase separation in the latter.

I. INTRODUCTION

The magnetic properties of T_L-T_E binary alloys (where T_L is a late-transition metal and T_E is an early-transition metal) are interesting because the magnetic moments of the glassy alloys are often higher than those of their corresponding equilibrium crystalline compounds.[1-3] As an example, saturation moment data for Co-Nb alloys[1,2] are plotted in Fig. 1. It is seen that Buschow's[1] moment data are higher than those of Naka *et al.*,[2] but both sets of data for the moments of the glasses are higher than those of the corresponding crystalline states. The difference between the data of Buschow[1] and Naka *et al.*[2] may have been caused by the different quench techniques that were used. Buschow and his co-workers[1,4,5] have suggested that the difference in moments between the glassy and the crystalline alloys are caused by chemical ordering in the glass such that like-atom bonding is preferred.

Chemical phase separation has been observed in Pd-Au-Si glasses,[6] in Zr-Ti-Be glasses,[7] in Pb-Sb-Au glasses,[8] in rare-earth glasses,[9] in Fe-Ni-B glasses,[10,11] and in Zr-Ni-B glasses.[12] Polymorphism in Ni-P glasses has been seen.[13] There is increasing evidence of chemical ordering in Fe-Zr glasses.[14] A recent study has shown that glassy Ni-P is chemically ordered, but that glassy Cu-Zr is not.[15] Unfortunately, neither Buschow,[1] nor Naka *et al.*[2] performed any structural analysis to check for chemical phase separation in their materials.

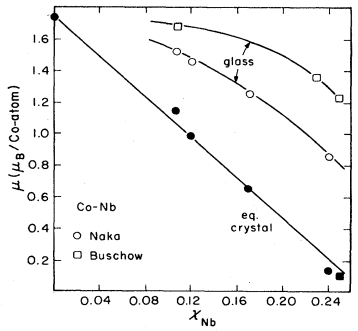

FIG. 1. Magnetic moments vs concentration (atomic fraction) for Co-Nb glasses (open symbols) and equilibrium crystalline specimens (solid).

The purpose of our work is to investigate the dependence of local structure and magnetism in glassy and crystalline Co-Nb-B alloys formed by liquid quenching. New data and models are presented so as to unify work done previously.[16-22] In Sec. II the experimental techniques are described. The results are given in Sec. III. In Sec. IV the results are analyzed in terms of a local environment model for the behavior of the magnetic moment as a function of composition. In Sec. V the conclusions are drawn.

II. EXPERIMENTAL PROCEDURES

The Co-Nb-B glasses were formed by rapid quenching from the melt with the usual melt-spinning technique. One alloy, $Co_{80}Nb_{12}B_8$, was formed with the ultrasonic gas atomization (USGA) technique.[22] The metal-spun ribbons had an average thickness of about 40 μm, the USGA powder had an average diameter of about 70 μm. The samples were analyzed by x-ray diffraction with Mo K_α radiation for maximum penetration. Crystallization of the glasses was performed by holding the samples at 700 °C for 2 h in a helium atmosphere. Specimens for scanning transmission electron microscopy (STEM) were made by the twin-jet electropolishing method. Ion milling the STEM specimens induced crystallization. Differential scanning calorimetry was made with a commercial instrument with a scan rate of 20 K/min. Magnetization measurements were made with a vibrating sample magnetometer with a temperature range of 77 to 1000 K. Values of the saturation magnetization at 0 K were obtained by extrapolating the saturation magnetization data to 0 K.

III. EXPERIMENTAL RESULTS

Most of the Co-Nb-B glasses formed rather easily by the melt-spinning method. The structures of the as-quenched ribbons are given in Table I. The compositions

TABLE I. As-quenched and crystallized structures of Co-Nb-B melt-spun alloys. The phases in parentheses [e.g., (Co_3Nb)] are less predominant phases by volume. Compositions are in atomic percent after analysis. ND represents not determined.

Composition (at. %)			As-quenched	Crystallized	T_x
Co	Nb	B	structure	structure	(°C)
80	6	14	fcc		
80	8	12	glassy	fcc	440
80	10	10	glassy	fcc (Co_2NbB)	445
80	12	8[a]	fcc		
80	12	8	glassy	fcc (Co_2NbB)	455
80	14	6	glassy	fcc (Co_3Nb)	470
80	15	5	glassy	fcc (Co_3Nb)	475[b]
80	18	2	glassy	Co_3Nb (fcc)	525[b]
80	20	0	fcc (Co_3Nb)	Co_3Nb (fcc)	
84	6	10	fcc		
84	10	6	glassy	ND	425
84	12	4	glassy	ND	450[b]
84	14	2	glassy (fcc)	ND	475[b]

[a]This composition was made by USGA.
[b]Estimated from the magnetization vs temperature curve.

are those obtained from chemical analysis. Figure 2 shows a ternary phase map of the as-quenched alloys along with the primary equilibrium phases.[23–25] In some cases, the specimens were crystalline, or partially crystalline, as-quenched. However, even the "glassy" samples may contain up to 5—10 vol. % microcrystallites.[17,26]

A micro-x-ray-fluorescence analysis was performed with the STEM on the $Co_{80}Nb_{14}B_6$ alloy to check for chemical phase separation in the glass. The smallest region that could be analyzed was about 100 Å. Parts of the latter sample were found to have 5—10 μm size domain patterns, where the Nb concentration was found to be roughly 15% higher along the domain borders than that found inside the domains. Piller and Haasen[10] have seen chemical separation with sizes of around 4 μm, but the compositional differences seen by the latter authors were much greater than that seen in this work. It is therefore unlikely that the Co-Nb-B glass is chemically separated enough for it to be classified as such.

Fixed-field thermomagnetic curves for the $Co_{80}Nb_xB_{20-x}$ series glasses are shown in Fig. 3. The crystallization temperatures as measured by differential scanning calorimetry (DSC) (arrows) are close to regions where the magnetization rises sharply. The saturation magnetizations for the $Co_{80}Nb_xB_{20-x}$ and the $Co_{84}Nb_xB_{16-x}$ glasses and crystalline specimens are listed in Table II, along with the extrapolated 0-K moments in Bohr magnetons. To evaluate the cause of the differences in moment ($\Delta\mu$) between the crystalline and glassy $Co_{80}Nb_xB_{20-x}$ alloys, an x-ray analysis was performed to identify the predominant phases in the crystallized alloys, and the results are listed in Table I. For alloys with $x \leq 12$, in which $\Delta\mu$ is 0.1 μ_B/Co-atom or less, it was found that the crystalline alloys were mostly fcc. However, for $x \geq 14$, in which $\Delta\mu$ is appreciably larger, the Co_3Nb phase, with the $MgNi_2$ structure,[27] was found. Other workers have reported the latter structure in binary Co-Nb (Ref. 28). Crystallized samples with $x=10$ and $x=12$ also had the Co_2NbB phase.[28]

IV. DISCUSSION

A. Magnetic moment models

Corb *et al.*[16] have used a ligand approach to model the magnetic moment in T_L-M alloys where M represents

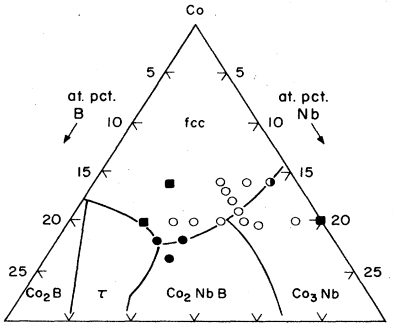

FIG. 2. Ternary phase map of the Co-Nb-B system showing results of rapid quenching. Open circles: glasses; solid circles: crystalline; squares: fcc. Predominant equilibrium crystalline phases (lines) are also shown (Ref. 23).

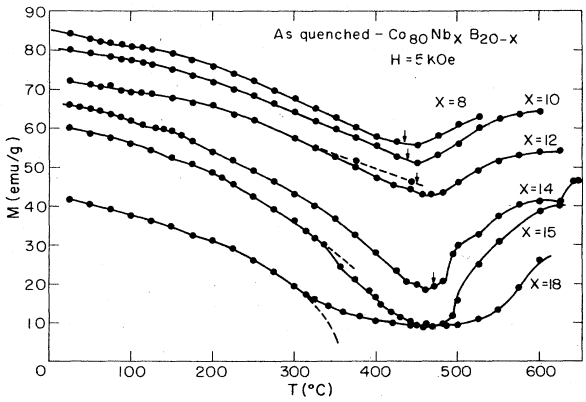

FIG. 3. Magnetization vs temperature for Co-Nb-B glasses. Arrows mark the crystallization temperatures as measured by DSC.

TABLE II. Magnetizations for Co-Nb-B alloys. M_s is the saturation moment in emu/g at temperatures shown in the parentheses in units of K. Saturation moments extrapolated to O K, μ, are given in Bohr magnetons per Co atom. ND represents not determined.

Composition (at. %)			glass			crystalline			
Co	Nb	B	M_s (293)	M_s (77)	M_s (0)	M_s (293)	M_s (77)	μ_{glass}	$\mu_{crystalline}$
80	6	14[a]				93.5	96.5		1.17
80	8	12	84	89	90	84.5	88.5	1.13	1.13
80	10	10	80	85	85	79	82	1.10	1.06
80	12	8[a,b]				ND	81		1.07
80	12	8	72	78	79	72	75	1.05	0.99
80	14	6	66	72.5	75	62	64.5	1.02	0.88
80	15	5	60	67	69.5	56	58.5	0.96	0.81
80	18	2	41.5	51	53	41	42.5	0.76	0.61
80	20	0[a]				39	43		0.65
84	10	6	92	95	96	ND	ND	1.23	ND
84	12	4	82	88	89	ND	ND	1.17	ND
84	6	10[a]				ND	109		1.32
84	14	2[c]	56	65	67	ND	ND	0.91	ND

[a]Mostly fcc as-quenched.
[b]USGA specimen.
[c]Partially crystalline as-quenched.

metalloid. In this model, it is assumed that the M atoms reduce the magnetic moments of neighboring T_L atoms by forming localized p-d bonds that reduce the number of spin-polarizable d orbitals on the T_L atoms. The result for the moments, in Bohr magnetons per T_L atom is

$$\mu = n_B - Z_M^{T_L}(n_B/5)X_M/X_{T_L} . \quad (1)$$

Here, n_B is the moment of the T_L atom in the pure state, $Z_M^{T_L}$ is the coordination number of T_L atoms around the M atoms, and X_M and X_{T_L} are the concentrations of M and T_L atoms where $\sum X_i = 1$. For the Co-B glasses, $Z_M^{T_L}$ is found to be 6,[16,29] in agreement with that found in the equilibrium Co_3B compound (Fe_3C structure), and also with that found by NMR[30,31] and by x-ray diffraction[32] in T_L-M glasses.

Although many T_E atoms in bcc Fe-T_E alloys carry non-negligible moments, such as Fe-Cr (Refs. 33 and 34) and Fe-V (Ref. 35), such is not the case for Co-T_E alloys. Neutron diffraction has shown that the moment reduction in Co-T_E alloys, where T_E=Cr and V (Refs. 34, 36, and 37) and T_E=Y (Ref. 38), occurs mostly by the reduction in moment of the Co atoms surrounding the T_E atoms. These and other experimental studies[39–43] have shown that the moment perturbation around a T_E atom extends out to at least three or four near-neighbor shells. We suppose that each T_E solute atom reduces the moment of each T_L atom in the ith coordination shell around the T_E atom by $g(r_i)$. The moment per T_L atom is then

$$\mu = n_B - \sum_{i=1}^{m} Z_{T_E}^{T_L}(r_i)g(r_i)(X_{T_E}/X_{T_L}) , \quad (2)$$

where $Z_{T_E}^{T_L}(r_i)$ is the coordination number of T_L atoms around a T_E atom at the ith coordination shell with distance r_i. For a random solid solution, we have

$$Z_{T_E}^{T_L}(r_i) = Z_{T_E}^{0}(r_i)X_{T_L} , \quad (3)$$

where $Z_{T_E}^{0}(r_i)$ is the total coordination number of shell i. Hence,

$$\mu = n_B - \sum_{i=1}^{m} Z_{T_E}^{0}(r_i)g(r_i)X_{T_E} . \quad (4)$$

To obtain the $g(r_i)$'s we fit the low-angle neutron scattering data of Cable and Hicks[36] for Co-V and Co-Cr fcc/hcp solid solutions with Marshall's[44] formula for the differential scattering cross section of unpolarized neutrons. We used three near-neighbor shells with Slater-type radial wave functions for the d electrons. The details are given in the Appendix.[45] The results for an fcc lattice are $g(r_i)=0.32$, $g(r_2)=0.07$, and $g(r_3)=0.053\mu_B/T_E$ atom.

In Fig. 4 the moments of various fcc/hcp Co-T_E alloys are plotted versus concentration for T_E=Ti (Refs. 46 and 47), Cr (Refs. 34, 48, and 49), V (Refs. 37 and 50) along with the result of Eq. (4) with the aforementioned param-

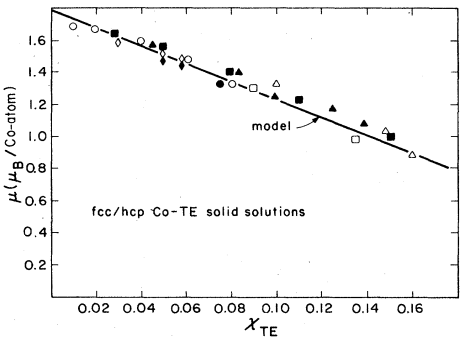

FIG. 4. Saturation magnetic moments vs composition (atomic fractions) for fcc/hcp Co-TE alloys. Co-Ti: open circles (fcc/hcp, Ref. 46), solid circles (fcc/hcp, Ref. 47). Co-Cr: open diamonds (fcc, Ref. 48), solid diamonds (hcp, Ref. 48), solid squares (hcp, Ref. 49), open squares (fcc, Ref. 34); Co-V: open triangles (close packed, Refs. 36 and 37), solid triangles (close packed, Ref. 50).

eters. The fit is quite good. The Jaccarino and Walker model[51] and the Friedel model[52] do not fit the data of Fig. 4 as well as Eq. (4).

An equation for the moment of a ternary T_L-T_E-M alloy can be easily formed by combining Eq. (1) and (2) as

$$\mu = n_B - Z_M^{T_L} n_B / 5(X_M / X_{T_L}) - \sum_{i=1}^{3} Z_{T_E}^{T_L}(r_i) g(r_i)(X_{T_E}/X_{T_L}) . \quad (5)$$

Following Cowley's treatment of chemical short-range ordering,[53] the coordination numbers can be written as

$$Z_M^{T_L} = Z_M^0 (X_{T_L} - \alpha_M^{T_E} X_{T_E} - \alpha_M^M X_M) , \quad (6a)$$

$$Z_{T_E}^{T_L}(r_i) = Z_{T_E}^0(r_i)(X_{T_L} - \alpha_{T_E}^M X_M - \alpha_{T_E}^{T_E} X_{T_E}) . \quad (6b)$$

The short-range order parameters, α_k^j, are defined such that a positive value is indicative of clustering of atom k around atom j, a zero value is indicative of random ordering, and a negative value indicates anticlustering between atoms k and j. Note that for binary Co-B alloys, we took $\alpha_M^M = -1.0$ and $Z_M^0 = 6$ since this alloy forms the Fe_3C-type structure in which the M atoms do not touch each other.[16] For binary Co-T_E alloys (fcc), it was assumed that a regular solid solution exists, implying that $\alpha_{T_E}^{T_E} = 0$.

B. Application of the model to Co-Nb-B alloys

The saturation moments of $Co_{80}Nb_xB_{20-x}$ alloys are plotted in Fig. 5. For $x \geq 14$, the moments of the crystallized samples are lower than those of the glasses and the fcc specimens, while for $x \leq 12$ the moments are approximately equivalent within experimental error. From Table I it is seen that the alloys with $x \geq 14$ have significant amounts of the Co_3Nb Laves-type phase. Hence, it is possible that the moment differences between the glassy and the equilibrium crystalline alloys are caused by the formation of weakly ferromagnetic phases ($\mu = 0.15\mu_B/Co_3Nb$, Ref. 1) in the latter, and not necessarily by gross phase separation in the former.

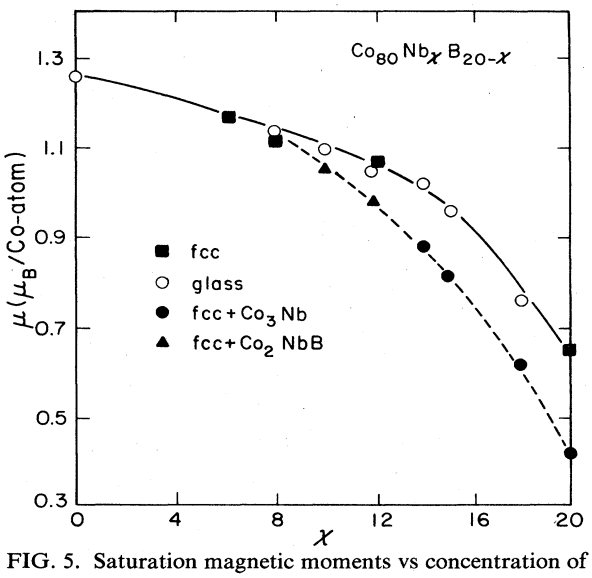

FIG. 5. Saturation magnetic moments vs concentration of Nb for Co-Nb-B specimens.

TABLE III. Fitting parameters used to model the magnetic data of the Co-Nb-B glasses.

Parameter	Value
n_B	1.79 μ_B/Co-atom
Z_M^0	6
$Z_{T_E}^0(r_1)$	12
$Z_{T_E}^0(r_2)$	6
$Z_{T_E}^0(r_3)$	24
$g(r_1)$	0.32 μ_B/T_E-atom
$g(r_2)$	0.07 μ_B/T_E-atom
$g(r_3)$	0.053 μ_B/T_E-atom
α_M^M	−1.0
$\alpha_{T_E}^{T_E}$	0.0
α	1.4

Because the moments of the glassy and fcc specimens are similar, the moments of these two alloy types can be modeled with Eqs. (5) and (6), using the parameters found in Sec. IV A for the Co-B and Co-T_E alloys, and by using $\alpha_M^{T_E}$ and $\alpha_{T_E}^M$ as fitting parameters. For this qualitative

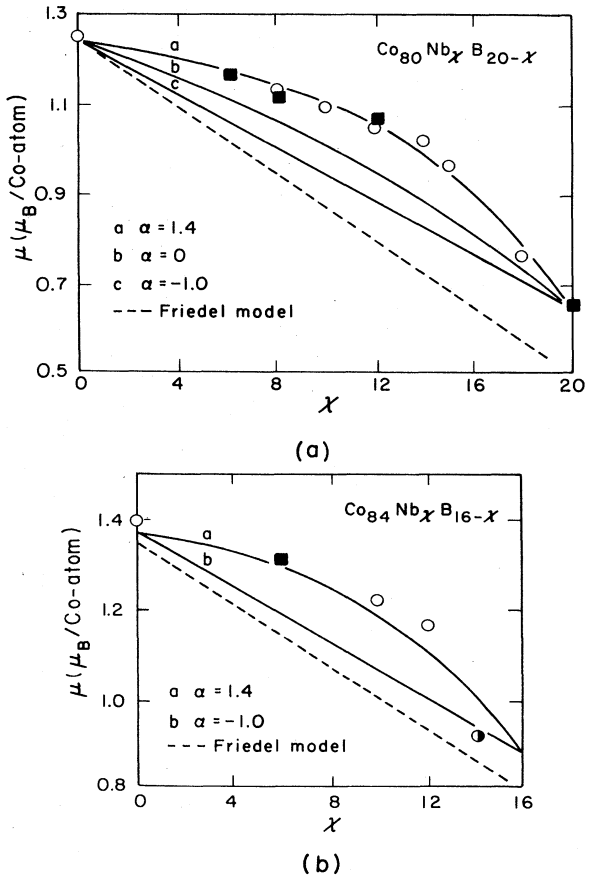

FIG. 6. Saturation magnetic moments vs concentration for glassy (circles) and fcc (squares) specimens of (a) $Co_{80}Nb_xB_{20-x}$ and (b) $Co_{84}Nb_xB_{16-x}$. The bond model is shown in dark lines for several values of α.

discussion we will take these two quantities as being equal and call them α. A fit of Eqs. (5) and (6) with the parameters listed in Table III to the moments of the fcc and glassy $Co_{80}Nb_xB_{20-x}$ alloys is shown in Fig. 6(a). The best fit is obtained with $\alpha=1.4$, and this value can be used to satisfactorally fit the glassy and fcc $Co_{84}Nb_xB_{16-x}$ moment data as shown in Fig. 6(b). Thus, B and Nb atoms have a tendency to cluster around one another in these alloys, a result consistent with the large electronegativity difference and the large negative heat of formation between these two atomic types.[54] The Friedel model is linear with x and does not provide a good fit, probably because it fails to take short-range order into account. We note that the bond model with $\alpha=-1.0$, implying no B and Nb interaction, also is linear: In fact, only by including some solute atom interaction can one reproduce the *curvature* seen in the data of Fig. 6.

The moments of the fcc and of the glassy samples are similar; therefore, it is possible that the solute atom coordination is also similar in these two structures, i.e., with B having 6 and Nb having 12 first near neighbors (Table III). The B environment in the glass could be similar to that of the Co_3B compound (with trigonal prismatic symmetry) or to that of an interstitial Co-B fcc solid solution (with octahedral symmetry). However, it appears that the coordination around the Nb atoms in the glass is quite different from that found in the equilibrium Co_3Nb Laves-type phase, since the latter structures have T_E atom coordination number of 16 or more.

V. CONCLUSIONS

From the magnetic data presented here, it is concluded that the differences in magnetic moments between the glassy and the equilibrium crystalline Co-Nb-B alloys are caused by the appearance of weakly ferromagnetic Laves-type phases in the latter, rather than by chemical phase separation in the former. By fitting the moment data of the glassy and the fcc specimens to a local environment model it was found, for both structures, that the coordination number around the Nb and B atoms is 12 and 6, respectively, and that the latter two atoms have a tendency to cluster around one another. It was numerically shown that clustering between the solute atoms causes the moment data to be nonlinear with composition.

ACKNOWLEDGMENTS

The authors are pleased to acknowledge support from the National Science Foundation, the Office of Naval Research (U.S. Department of the Navy), and the Army Research Office (U.S. Department of the Army). Dr. Tony Garrett-Reed is thanked for his help with the STEM work.

APPENDIX

To evaluate the $g(r_i)$'s the following procedure was used. The differential cross section for the magnetic diffuse scattering of unpolarized neutrons is, following Marshall,[44]

$$d\sigma/d\Omega=53.0f^2(k)X_{T_E}X_{T_L}M^2(k)\ , \tag{A1}$$

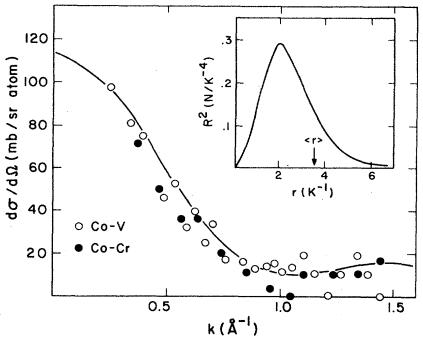

FIG. 7. Differential neutron scattering cross sections vs wave vector k for fcc Co-5 at.%V (open circles) and fcc/hcp Co-5%Cr (closed). The line is the best fit to the data as described in the Appendix. The inset shows the probability density of the Slater function, $R^2(r)$ vs r (expressed in units of the normalization constant, N, and the parameter K).

where the cross section is given in mb/sr/atom, $f(k)$ is the unpaired d-electron form factor for the Co atom and it is taken as $f(k)=\exp(-0.05k^2)$ (Ref. 37). $M(k)$ is

$$M(k)=\mu_{T_E}-\mu_{T_L}-X_{T_L}\sum_1^m Z^0_{T_E}(r_i)g(r_i)\frac{\sin(kr_i)}{(kr_i)}\ . \tag{A2}$$

Here, k is the magnitude of the scattering vector, and the other terms are defined in the text. We will take $m=3$, and for a substitutional fcc lattice we have $Z^0_{T_E}(r_1)=12$, $Z^0_{T_E}(r_2)=6$, and $Z^0_{T_E}(r_3)=24$. The r_i's are determined by the fcc Co lattice parameter of $a_0=3.5447$ Å.

Diffuse neutron data of Cable and Hicks[36] is shown in Fig. 7 for 5% solid solutions of Co-V and Co-Cr. The moment difference, $\mu_{T_E}-\mu_{T_L}$, is easily found by extrapolation to large values of k and the result is $-1.4\mu_B$/atom. Now there are three unknowns to fit Eqs. (A1) and (A2) to one graph. To reduce the number of variables to the fit, a Slater function for the radial component of a d electron is assumed,

$$R(r)=\left[\frac{(2K)^7}{4\pi 6!}\right]^{1/2} r^2\exp(-Kr)\ , \tag{A3}$$

where the term in large parentheses is obtained by normalization such that $\int_0^\infty R^2(r)d\Omega=1.0$. The expectation value $\langle r\rangle$ is 3.5 K^{-1}. We will define $r_1=\langle r\rangle$ so that we obtain $K=1.397$ Å^{-1}. The probability density, $R^2(r)$, for the d electrons has a large peak roughly centered between the central atom and its first near neighbors, as seen in the inset of Fig. 7. This is probably representative of the solid since the dilute T_E impurities produce very narrow, localized states in the density of states.[45] The $g(r_i)$'s are now obtained by scaling as

$$g(r_i)=g(r_1)R^2(r_i)/R^2(r_1)\ . \tag{A4}$$

Only one fitting parameter is left, namely $g(r_1)$. The best fit to the data of Fig. 7 is obtained with $g(r_1)=0.32\mu_B/T_E$ atom and thus from Eq. (A4) we have $g(r_2)=0.07$ and $g(r_3)=0.053\mu_B/T_E$ atom. These parameters can be used to fit the Co-V and the Co-Cr data equally well.

*Present address: Institut für Physik der Universität Basel, Klingelbergstrasse 82, CH-4056 Basel, Switzerland.
[1]K. H. J. Buschow, J. Appl. Phys. **53**, 7713 (1982).
[2]M. Naka, N. S. Kazama, H. Fujimori, and T. Masumoto, in *Proceedings of the 4th International Conference on Rapidly Quenched Metals,* edited by T. Masumoto and K. Suzuki (Japanese Institute of Metals, Sendai, 1982), p. 919.
[3]K. H. J. Buschow, M. Brouha, J. W. M. Biesterbos, and A. G. Dirks, Physica (Utrecht) **91B**, 261 (1977).
[4]K. H. J. Buschow and P. G. Van Engen, J. Appl. Phys. **52**, 3557 (1981).
[5]A. M. Van der Kraan and K. H. J. Buschow, Phys. Rev. B **25**, 3311 (1982).
[6]C.-P. Chou and D. Turnbull, J. Non-Cryst. Solids **17**, 169 (1975).
[7]L. E. Tanner and R. Ray, Scr. Metall. **14**, 657 (1980).
[8]S. T. Hopkins and W. L. Johnson, Solid State Commun. **43**, 537 (1982).
[9]C. O. Kim and W. L. Johnson, Phys. Rev. B **23**, 143 (1981).
[10]J. Piller and P. Haasen, Acta. Metall. **30**, 1 (1982).
[11]P. Haasen, J. Non-Cryst. Solids **56**, 191 (1983).
[12]A. Mak, K. Samwer, and W. L. Johnson, Phys. Lett. **98A**, 353 (1983).
[13]D. S. Lashmore, L. H. Bennett, H. E. Schone, P. Gustafsor, and R. E. Watson, Phys. Rev. Lett. **48**, 1760 (1982).
[14]K. Shirakawa, K. Fukamichi, T. Kaneko, and T. Masumoto, Physica (Utrecht) **91B**, 192 (1983); V. Mizutani, M. Matsuura, and K. Fukamichi, J. Phys. F (to be published).
[15]R. Harris and L. J. Lewis, J. Phys. F **13**, 1359 (1983).
[16]B. W. Corb, R. C. O'Handley, and N. J. Grant, Phys. Rev. B **27**, 636 (1983).
[17]B. W. Corb, R. C. O'Handley, J. Megusar, and N. J. Grant, Phys. Rev. Lett. **51**, 1386 (1983).
[18]R. C. O'Handley, B. W. Corb, Y. Hara, N. J. Grant, and W. Hines, J. Appl. Phys. **53**, 7753 (1982).
[19]R. C. O'Handley and N. J. Grant, in *Rapidly Solidified Amorphous and Crystalline Alloys,* edited by B. H. Kear and B. C. Giessen (Elsevier, New York, 1982), p. 217.
[20]B. W. Corb, R. C. O'Handley, S. Paradies, and N. J. Grant, J. Appl. Phys. **55**, 1781 (1984).
[21]B. W. Corb, R. C. O'Handley, N. J. Grant, and V. Moruzzi, J. Magn. Magn. Mater. **31-34**, 1537 (1983).
[22]R. C. O'Handley, P. Domalavage, B. W. Corb, Y. Hara, and N. J. Grant, in *Rapid Solidification Processing, Principles and Technologies, III,* edited by R. Mehrabian (Natl Bur. Stand., Gaithersburg, Md., 1983), p. 678.
[23]H. H. Stadelmaier and J.-D. Schöbel, Metall **20**, 31 (1966).
[24]H. H. Stadelmaier and G. Hofer, Metall **18**, 460 (1964).
[25]H. H. Stadelmaier, J.-D. Schöbel, and R. A. Jones, Metall **21**, 17 (1967).
[26]J. Megusar and N. J. Grant, Mater. Sci. Eng. **49**, 275 (1981).
[27]W. B. Pearson, *The Crystal Chemistry and Physics of Metals and Alloys* (Wiley, New York, 1972), p. 643.
[28]F. W. J. Pargeter and W. Hume-Rothery, J. Less-Common Met. **12**, 366 (1967); H. Sato and H. Beck, Trans. Metall. Soc. AIME **218**, 670 (1960).
[29]R. Hasegawa and R. Ray, J. Appl. Phys. **50**, 1586 (1979).
[30]P. Panissod, I. Bakonyi, and R. Hasegawa, Phys. Rev. B **28**, 2374 (1983).
[31]J. Durand and P. Panissod, IEEE Trans. Magn. **MAG-17**, 2595 (1981).
[32]D. S. Bourdreau and H. J. Frost, Phys. Rev. B **23**, 1506 (1981).
[33]A. T. Aldred, B. D. Rainford, J. S. Kouvel, and T. J. Hicks, Phys. Rev. B **14**, 228 (1976).
[34]C. G. Shull and M. K. Wilkinson, Phys. Rev. **97**, 304 (1955).
[35]M. Hennion, J. Phys. F **13**, 2351 (1983). This author quotes data from the following reference: O. Yamashita, Y. Yamagushi, and H. Watanabe, in *Annual Progress Report on Neutron Scattering Studies in JAERI, 1981,* p. 61 (unpublished).
[36]J. W. Cable and T. J. Hicks, Phys. Rev. B **2**, 176 (1970).
[37]J. W. Cable, J. Appl. Phys. **53**, 2456 (1981).
[38]A. Oppelt and K. H. J. Buschow, Phys. Rev. B **13**, 4698 (1976).
[39]M. F. Collins and G. G. Low, Proc. Phys. Soc. London **86**, 535 (1965).
[40]T. M. Holden, J. B. Comly, and G. G. Low, Proc. Phys. Soc. London **92**, 726 (1967).
[41]A. T. Aldred, B. D. Rainford, T. J. Hicks, and J. S. Kouvel, Phys. Rev. B **7**, 218 (1973).
[42]K. Levin and D. L. Mills, Phys. Rev. B **9**, 2354 (1974).
[43]M. B. Stearns, Phys. Rev. B **13**, 1183 (1976).
[44]W. Marshall, J. Phys. C **1**, 88 (1968).
[45]F. U. Hillebrecht, J. C. Ruggle, G. A. Sawatztky, and R. Zeller, Phys. Rev. Lett. **51**, 1187 (1983).
[46]W. S. Chan, K. Misuoka, H. Miyama, and S. Chikazumi, J. Phys. Soc. Jpn. **48**, 822 (1980).
[47]G. Suran, J. Sztern, J. A. Aboaf, and T. R. McGuire, IEEE Trans. Magn. **MAG-17**, 3065 (1981).
[48]J. Crangle, Philos. Mag. **2**, 659 (1957).
[49]F. Bolzoni, F. Leccabue, R. Panizzieri, and L. Pareti, J. Magn. Magn. Mater. **31-34**, 845 (1983).
[50]Y. Aoki and M. Yamamoto, Phys. Status Solidi A **33**, 625 (1976).
[51]V. Jaccarino and L. R. Walker, Phys. Rev. Lett. **15**, 258 (1965).
[52]A. P. Malozemoff, A. R. Williams, K. Tarakura, V. L. Moruzzi, and K. Fukamichi, J. Magn. Magn. Mater. **35**, 192 (1983).
[53]J. M. Cowley, Phys. Rev. **77**, 669 (1940).
[54]A. R. Miedema, J. Less-Common Met. **46**, 67 (1976).